Mathematical Modeling of the Origami Navel Shell

Gurmeher Kaur[1], Crystal Soong[1], and Jasleen Kaur[#]

[1]Chapel Hill High School, Chapel Hill, NC, USA
[#]Advisor

ABSTRACT

The well-known Nautilus shell has been modeled extensively both by mathematicians and origamists. However, there is wide disagreement on the best-fitting mathematical model — partly because there is significant variability across different Nautilus Shells found in nature, and no single model can describe all of them well. Origami structures, however, have precise repeatable folding instructions, and do not exhibit such variability. Ironically, no known mathematical models exist for these structures. In this research, we mathematically model a prominent origami design, the Navel Shell by Tomoko Fuse, believed to be based on the Nautilus. We use first-principles geometric and trigonometric constructs for developing a non-smooth Geometric Model of the ideal origami spiral. We then search for the best-fitting parametric smooth spiral approximation, by formulating the fitting problem as a minimization problem over four unknowns. We write a Python computer program for searching the space numerically. Our evaluations show that: (i) the Smooth spiral is an excellent fit for the Geometric Model; (ii) our models for Origami Navel Shell are different from prior mathematical models for the Nautilus shell, but they come close to a recent model for a rare species of Nautilus; (iii) the Geometric Model explains the outer edges of origami images quite well and helps identify construction errors in the inner edges; and (iv) the Smooth Model helps understand how well the ideal Navel Shell matches different variants of the Nautilus species. We hope our research lays the foundation for further mathematical modeling of origami structures.

Introduction

Modeling of the shape of artifacts foun incorporated in nature is useful to scientists — shape modeling in the scientific world has already led to many discoveries and innovations [7][8][32][41]. For example, it can help scientists discover and understand biological processes [32]. Medical image processing technology can help doctors understand the normal shape of an organ, which can be useful for early diagnosis and treatment [41]. Another example includes sunflower centers, a product of millions of years of evolution, with an extremely efficient arrangement of seeds. Modeling these centers have helped scientists find extremely compact and efficient ways to model other objects [7].

One of the shapes that has generated keen interest in the mathematical world is the *spiral,* which is abundant in nature: galaxies, tornadoes, hurricanes, flowers, and shells [29]. Shells, in particular, have been studied for long, and mathematical models [44] and origami designs [29] have been developed for these. In particular, the well-known *Nautilus* shell has been widely studied because of its exquisite chambers and logarithmic spiral shape [25].

There have been many mathematical models proposed for the Nautilus shell. A few sources, including blogists, artists, and novelists, claim that the Nautilus is an example of a Golden Spiral [6][12][22][34][36], which is a well-known logarithmic spiral that grows by the Golden Ratio ($\varphi \approx 1.618$) every 90°. However, most mathematicians disagree with this claim [11][13][14][15][19][20][23][26][27][28][35][39][40]. In general, while mathematicians agree that the Nautilus shell is a logarithmic spiral, they widely disagree on the type of logarithmic spiral. Some claim that the growth *rate* of the Nautilus is different from the Golden Ratio, φ, while others claim that the *angle* of growth is different from that of a Golden Spiral. For example, [28] states that when a spiral grows by the ratio φ every 180° (instead of 90°), it fits Nautilus shells much better. This, however, is contradicted by others, including

[4][11][14][19][26][28][35]. We believe that one of the reasons for such wide disagreement among mathematical models is the *variability* across different Nautilus found in nature [28] — no two Nautilus shells are the same; so a model that fits one shell, may not fit another. Because of the variability, we wonder — is it even possible to create a single model that fits all Nautilus Shells?

In contrast, several origami structures have also been designed to model the Nautilus Shell, which *do* have very precise repeatable folding instructions [23][44]. The preciseness of the instructions stands in stark contrast to the variability found among real Nautili. Unfortunately, to the best of our knowledge, the preciseness of the instructions has not been exploited by anyone before to come up with a mathematical model for origami structures of the Nautilus [19]. In this project, we fill this gap.

Specifically, we pick the Origami Navel Shell designed by Tomoko Fuse [16], which is believed to be based on the Nautilus. Using a first principles approach, we mathematically model this origami structure. Our methodology relies on geometric modeling of the folding instructions, as well as curve-fitting to find the smooth spiral that best explains the ideally-constructed Origami Navel Shell. Our models help mathematically understand the shape of the Origami Navel Shell, as well as understand its relation to the Nautilus Shell.

In the rest of this paper, we formulate our research question in Section 2, develop our geometric model for the Origami Navel Shell in Section 3, and a smooth spiral approximation in Section 4. We validate our models in Section 5, study their relation to the state of the art in Section 6, summarize our limitations and future directions in Section 7, and our conclusions in Section 8. Photo credits for all images included in the paper are listed just before the bibliography.

Formulating The Research Question

We initially attempted to find online images of already constructed Origami Navel Shells, and then tried to study what curve would fit them the best. We were motivated by several references, including [38][28][25][30][35], that stated that a logarithmic curve could fit the Nautilus Shell, although they disagree on the exact logarithmic curve. Our hope was that one of these models might explain an Origami Navel Shell well.
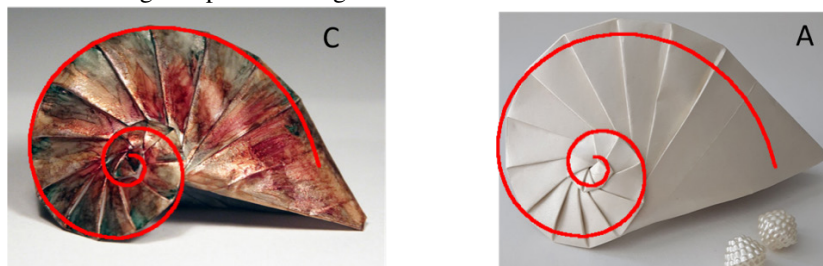

Fig. 1: The same logarithmic spiral does not fit different images of Origami Navel Shells[1]

After experimenting with several origami images and proposed models for a Nautilus Shell, however, we found that a spiral that fits one origami image well, throughout inner and outer curves, may not fit another well at all (see Figure 1). We believe that this disparity is due to two main factors: (i) the variability introduced due to human error when folding the spiral, and (ii) the distortion introduced by a non-orthogonal angle of photography and non-flat structure. First, every individual person has a slightly different (imprecise) way of folding the spiral even if we all tried to follow the same instructions – so the constructed structures would have small differences in them. Second, if the constructed origami structure is not well flattened onto a two-dimensional plane, and/or if the angle of photography is not perpendicular to such a plane, then the photograph will be a non-orthogonal two-dimensional projection of the

---

[1] The A and B labels in the images refer to photo credits, which are listed prior to bibliography.

origami spiral, which can lead to distortions. Based on this, we realized that photographs taken by humans of human-made origami spirals will likely not be an accurate data source.

However, the folding instructions for the origami spiral *are* precise and freely available – starting from a square, several successive folding instructions lead to the origami structure. We hypothesized that we could analyze the folds in an Origami Navel Shell, and then use first principles of geometry and trigonometry to derive what the side lengths and angles are supposed to be in a *precisely* constructed structure. If successful, this would allow us to construct a geometric model of the *ideal* Origami Navel Shell. We could then fit a smooth spiral on to this geometric model, in order to find the spiral that best models the Origami Navel Shell. In the next two sections, we use this approach for developing our geometric and smooth models.

Geometric Modeling

Although we found photographs of several different types of origami models for the Nautilus Shell [43][44][23], the only one where instructions were readily available was the popular model by the prominent origamist, Tomoko Fuse [16][18][43]. Throughout this section, we use these instructions to derive our model of Fuse's Origami Navel Shell.
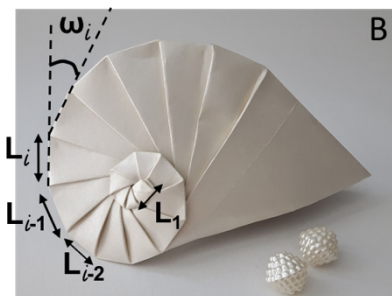

Fig. 2: Geometric modeling goal: derive $\{L_i, \omega_i\}$

By examining Fuse's finished Origami Navel Shell, we see that there are three features of the spiral that are determined by the folding instructions. These include the outer edge lengths, the angles between the outer edges, and the radial lines coming in from the outer edges. Unfortunately, these radial lines do not meet at a single point (unlike most mathematical spirals, where the radial lines meet at the center of the spiral) – therefore, it is not clear how useful they would be in relating the origami spiral to a mathematical spiral. So, for the purpose of developing our geometric model, we instead focus on the lengths of and angles between the outer spiral edges (Figure 2). We describe our methodology for modeling both of these below.

The Outer Edge Lengths, L_i

Fuse's folding instructions first fold two sides of a square along a diagonal to create a kite shaped structure, as shown in Figure 3.[2] The triangle ABC gets folded along CA to form ADC. The next series of steps involve creating horizontal creases along the bottom folded triangle of the kite. This is done in two phases.

---

[2] Most geometric figures in this paper have been drawn to scale using the GeoGebra software [5].
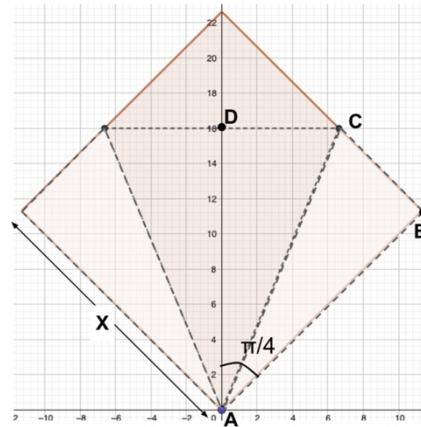
Fig. 3: Folding the original square to a kite shape

In the first phase, the top half of the folded triangle is folded in half multiple times to create eight equal-width horizontal sections in the top half of the folded triangle (see Figure 4(a)). If X represents the side length of the original square, then the width of these 8 sections is $\frac{X}{16}$. This is because the total height of the folded triangle is X, and it is divided by two every time it is folded.

In the second phase, the folding instructions require repeatedly folding the bottom tip of the kite shape up to 1½ widths of the horizontal sections starting from the top (see Figure 4(b)). Observe that the first horizontal section created in this second phase has a width of $(\frac{1}{2} * \frac{3}{2})$ of $\frac{X}{16}$. The widths of the remaining horizontal sections can be similarly derived.
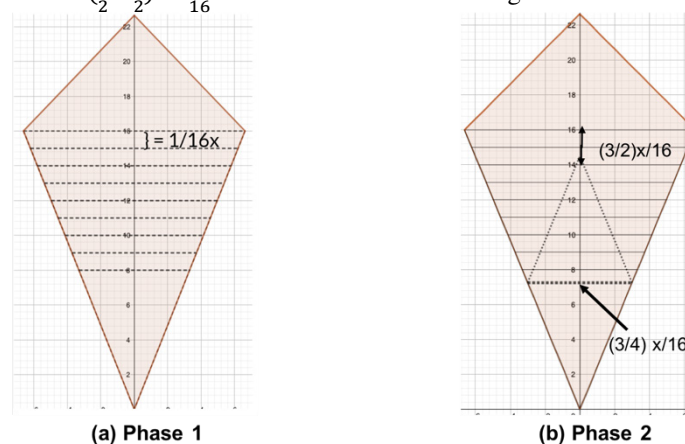

(a) Phase 1   (b) Phase 2

Fig. 4: Folding the horizontal sections

After completing the two phases, we get twenty horizontal sections with the following properties (see Figure 5(a)):

8 equal-width sections, each with a width of $X/16$.

5 equal-width sections, each with a width of $3/4$ of $X/16$.

3 equal-width sections, each approximately $(3/4)^2$ of $X/16$.

2 equal-width sections, each approximately $(3/4)^3$ of $X/16$.

1 section, with width of approximately $(3/4)^4$ of $X/16$.

1 section, with width of approximately $(3/4)^5$ of $X/16$.

Observations: *We note two interesting findings revealed by our modeling so far:*

The *number* of equal-width sections, counted from the bottom, follows the Fibonacci Sequence (1, 1, 2, 3, 5, 8, …). This is fascinating because the Fibonacci Sequence, in fact, lies at the basis of the construction of the famous Golden Spiral. Does this mean that the Golden Spiral models the Origami Navel Shell well?

The width of each group of equal-width sections grows by the ratio of 4/3 from the previous, starting at the bottom tip of the kite. Will this ratio of 1.33 play a role in the model developed for the Origami Navel Shell?
We will revisit these observations after deriving our models.

The Angles Between Outer Edges, ω_i

After creasing the horizontal sections of the triangle, we are instructed to make diagonal creases in each section, starting from the center line and going up to the top right corner of each section (as shown in Figure 5(b) and Figure 6).

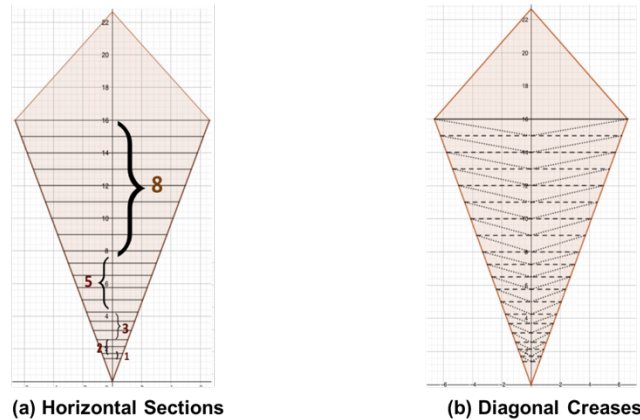**(a) Horizontal Sections**   **(b) Diagonal Creases**

Fig. 5: The completed horizontal and diagonal creases

For determining the angles between the spiral outer edges, we introduce the following notation. L_i represents the width of the ith section, starting from the bottom, H_i represents the length of the top horizontal edge of the ith section, and μ_i represents the angle made by the diagonal crease going from the bottom left to the top right of the ith section. After careful examination of the folds in origami structures we constructed, we realized that the angle μ_i (shown in Figure 6) determines the angle between the neighboring outer edges of the final folded spiral. Below, we elaborate how.

For folding the ith outer edge of the spiral, the bottom right tip (B_{i-1}) of the green triangle in Figure 6 is folded along the dashed diagonal crease ($A_{i-1}B_i$), resulting in the orange triangle. This implies that the angle between the outer edges L_i and L_{i-1} is $180° - 2*\mu_i$ (or with respect to Figure 2, $\omega_i = 2*\mu_i$). Therefore, our search for the angle between the outer edges of the constructed spiral boils down to determining the angle of μ_i for all twenty sections.
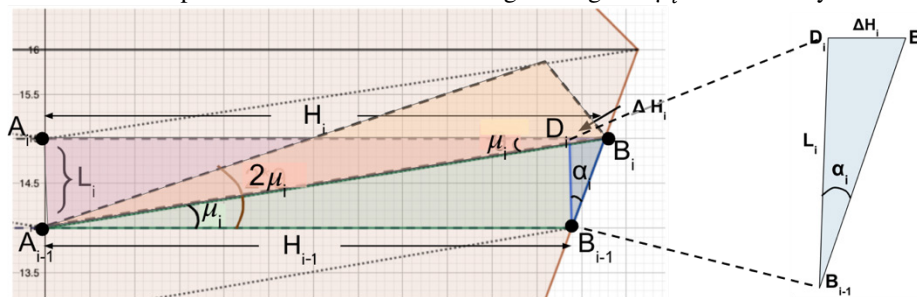

Fig. 6: The ith horizontal section

Lemma 1: In the ith section, $\mu_i = cot^{-1}\left(\frac{H_i}{L_i}\right)$.

Proof: A_iB_i and $A_{i-1}B_{i-1}$ (top and bottom horizontal edges of the ith section) are parallel segments. Based on the Alternate Interior Angles Theorem [33], we get: $\angle A_{i-1}B_iA_i = \mu_i$. In the right triangle $A_{i-1}A_iB_i$, we use the cotangent ratio of μ_i to get: $\mu_i = cot^{-1}\left(\frac{H_i}{L_i}\right)$. Hence, proved. □

In Section 3.A, we have already derived the values of L_i for all horizontal sections. For computing μ_i using Lemma 1, we also need the horizontal edge lengths H_i. We rely on the next lemma for that.

Lemma 2: $H_{i-1} = H_i - L_i * tan(\pi/8)$, $2 \leq i \leq 20$.

Proof: To establish the relationship between H_i and H_{i-1}, we amplify the right-angled triangle $B_{i-1}D_iB_i$, located at the right side of ith section (shown on the right of Figure 6). The top edge length of this triangle is given by $\Delta H_i = H_i - H_{i-1}$. We use the tangent ratio of α_i to get: $tan(\alpha_i) = \frac{\Delta H_i}{L_i}$.

In order to find out the value of α_i, we first consider the angle ∠DAC in Figure 3, and make two observations. First, when the original square is folded into a kite, the resulting triangles ABC and ABD are congruent. This is because edge lengths AB and AD are equal, BC and DC are equal, and AC is a common edge of both triangles (Reflexive property). From the SSS Triangle Congruence Theorem, the two triangles are congruent [33]. This implies that angle ∠BAC is equal to angle ∠DAC. Second, we know that angle ∠BAD is $\frac{\pi}{4}$ radians (or 45°), because the diagonal line of the square divides the right-angled vertex into two halves. Therefore, angle ∠DAC is $\frac{\pi}{8}$ radians.

Next, we establish that angle DAC is equal to angle $D_iB_{i-1}B_i$. Note that AD and $B_{i-1}D_i$ are parallel to each other (since both are perpendicular to the horizontal axis). The line segment AC (from Figure 3) intersects both of these. Based on the Corresponding Angles Theorem [33], we get: $\angle DAC = \angle D_iB_{i-1}B_i$. Hence, $\alpha_i = \angle D_iB_{i-1}B_i = \frac{\pi}{8}$ radians.

Substituting for α_i, we get: $tan\left(\frac{\pi}{8}\right) = \frac{\Delta H_i}{L_i}$. Thus, $H_{i-1} = H_i - L_i * tan(\pi/8)$. Hence, proved. □

Lemma 2 gives us a *recursive* relation for deriving H_{i-1} from H_i. The angle between the outer spiral edges in Figure 2 is given by: $\omega_i = 2 * \mu_i$. Lemma 3 below builds on Lemmas 1 and 2 to establish how to compute ω_i.

Lemma 3: The angle between the outer spiral edges is given by: $\omega_i = 2 \, cot^{-1}\left(\frac{H_i}{L_i}\right)$, where $\frac{H_{20}}{L_{20}} = 16 \, tan(\pi/8)$, and $\frac{H_{i-1}}{L_i} = \frac{H_i}{L_i} - tan(\pi/8)$, for all $2 \leq i \leq 20$.

Proof: In triangle ADC in Figure 3, DC = H_{20}, and AD = X, and angle ∠DAC is $\frac{\pi}{8}$ radians (established in proof of Lemma 2). In Section 3.1, we have already established that $L_{20} = X/16$. Hence, $tan(\pi/8) = \frac{H_{20}}{16 \, L_{20}}$, or $\frac{H_{20}}{L_{20}} = 16 \, tan(\pi/8)$.

From Lemma 2, we get: $\frac{H_{i-1}}{L_i} = \frac{H_i}{L_i} - tan(\pi/8)$, for all $2 \leq i \leq 20$.

From Lemma 1, we get: $\omega_i = 2 \, \mu_i = 2 \, cot^{-1}\left(\frac{H_i}{L_i}\right)$. Hence, proved. □

We use Lemma 3 to compute ω_i for all outer edges of the folded spiral.

The Complete Geometric Model

All of the computed values of L_i and ω_i are listed in Table 1. This completes our Geometric Model of an ideal construction of Fuse's Origami Navel Shell spiral. Figure 7 plots this model using the GeoGebra software [5].

i	L_i	H_i	ω_i	$\sum_{k=1}^{i} \omega_k$
1	45X/2048	143(√2-1)X/2048	74.45°	74.45°
2	53X/2048	49(√2-1)X/512	66.27°	140.72°
3	14X/512	63(√2-1)X/512	56.43°	197.15°
4	17X/512	40(√2-1)X/256	54.32°	251.47°
5	9X/256	49(√2-1)X/256	47.83°	299.30°
6	9X/256	29(√2-1)X/128	41.07°	340.37°

| 7	5X/128	17(√2-1)X/64	39.09°	379.46°
8	3X/64	20(√2-1)X/64	39.81°	419.27°
9	3X/64	23(√2-1)X/64	34.96°	454.23°
10	3X/64	26(√2-1)X/64	31.13°	485.36°
11	3X/64	29(√2-1)X/64	28.05°	513.41°
12	3X/64	8(√2-1)X/16	25.51°	538.92°
13	X/16	9(√2-1)X/16	30.03°	568.95°
14	X/16	10(√2-1)X/16	27.15°	596.10°
15	X/16	11(√2-1)X/16	24.76°	620.86°
16	X/16	12(√2-1)X/16	22.75°	643.61°
17	X/16	13(√2-1)X/16	21.04°	664.65°
18	X/16	14(√2-1)X/16	19.57°	684.82°
19	X/16	15(√2-1)X/16	1`	702.50°

Table 1: Specification of the Geometric Model
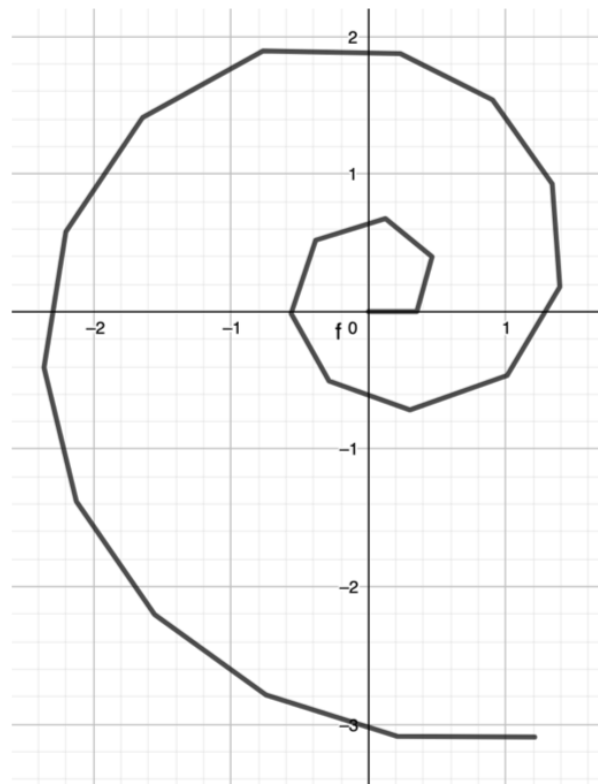
Fig. 7: The completed Geometric Model

Parametric Curve Fitting

Our Geometric Model is non-smooth. In this section, we find a parametric smooth spiral that approximates our Geometric Model well. This will also help us compare to previously proposed smooth models for the Nautilus Shell. Short-listing to a Logarithmic Spiral

We began to think about how to find a smooth spiral that approximates our Geometric Model. In order to shortlist the types of spirals to consider, we tried fitting prominent ones, including the Archimedean Spiral, the Golden Spiral, the Hyperbolic Spiral, and Fermat's Spiral [42].

As can be seen in Figure 8, the Archimedean Spiral and Fermat's Spiral grow too slow to fit our geometric model. The Hyperbolic Spiral, on the other hand, grows too fast. The Golden Spiral matches the inner vertices of our geometric model better than the others, but seems to grow fast for the outer vertices. The spiral of the Nautilus Shell, which the Origami Navel Shell is believed to be based on, is known to be a *logarithmic* spiral. The Golden Spiral is also a type of logarithmic spiral, with its own characteristic rate of growth – perhaps a logarithmic spiral with a smaller growth factor might be the smooth spiral that best fits our geometric model. In the rest of this section, we focus on the logarithmic spiral, and outline our search for finding the best-fitting one.
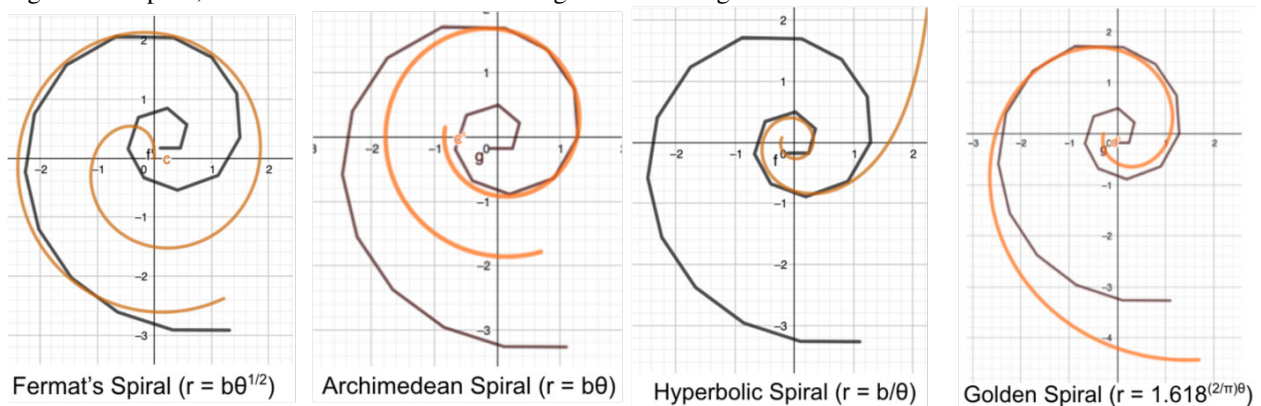

Fermat's Spiral (r = bθ^{1/2}) | Archimedean Spiral (r = bθ) | Hyperbolic Spiral (r = b/θ) | Golden Spiral (r = 1.618^{(2/π)θ})

Fig. 8: Fitting prominent mathematical spirals to our Geometric Model

The Four Unknown Parameters

The general polar equation of a logarithmic spiral is $r = a * e^{\theta * b}$, in which θ is the angle of rotation as the curve spirals, r is the radius corresponding to angle θ of the spiral, a is a constant that represents the scaling factor, b is a constant that represents the growth factor, and e is the base of the natural logarithm. The first two unknowns in our search for a smooth spiral that fits our Geometric Model well, therefore, are a and b.

However, from Tomoko Fuse's folding instructions, there is no obvious way to locate the center of the geometric spiral (the origin is typically the center of smooth mathematical spirals). Therefore, the problem of fitting a smooth spiral to our Geometric Model is also concerning the translation vector that must be applied to the Geometric Model in order to position it in the same coordinate space. The example in Figure 9 illustrates the role of the translation vector – it is clear that the translation in the first figure fits the Golden Spiral much better than in the second figure.
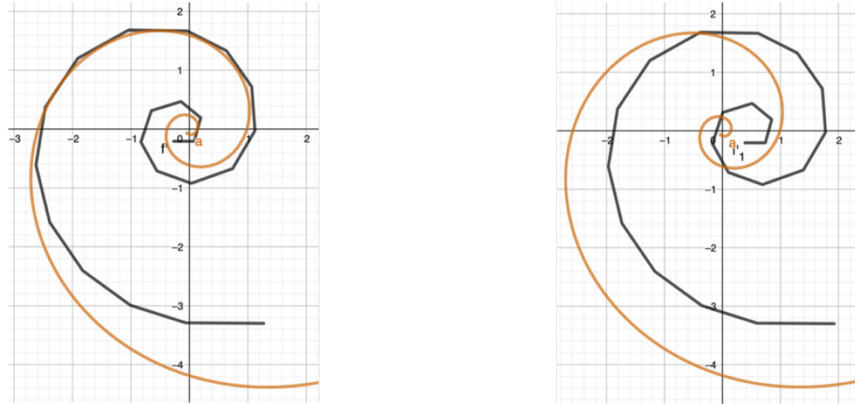
Fig. 9: Role of translation in finding the best fit

So, finding the best fitting logarithmic spiral boils down to searching for four unknowns; the x and y translates, (xT, yT), that must be applied to the Geometric Model, and the a and b that define the smooth logarithmic spiral. After trying a few combinations of the four unknowns, we soon realized that the search space for the four unknowns is too large for us to find the best fitting curve manually. So, instead, we develop a computer program that computationally searches through the space of the four unknowns.

Measuring the Goodness of Fit

In order to develop a numerical method for finding the best-fitting logarithmic spiral, we need to formulate a measure that captures how well-fitting a given smooth spiral is to our geometric model. It would be natural to use the *gaps* between the vertices of our Geometric Model and a given smooth spiral as a measure of the goodness of fit. But, how do we find out what is the gap between a given vertex and the smooth spiral?

   Vertical Gap (Cartesian Coordinates): One option is to rely on the Cartesian coordinates (x_i, y_i) of the twenty vertices of our Geometric Model, and for each x_i, compute the difference between y_i and the *y*-coordinate of that point on the logarithmic spiral, which lies at the intersection with the line $x = x_i$. This measure captures the *vertical* gap between the two spirals (Figure 10 (a)). However, we observed that this measure can significantly differ from the actual gap between the geometric model and smooth spiral – as the example in Figure 10 (a) shows, the vertical gap may be significantly larger for some vertices than the shortest gap between the vertex and the logarithmic spiral. Therefore, the vertical gap is an unreliable measure.
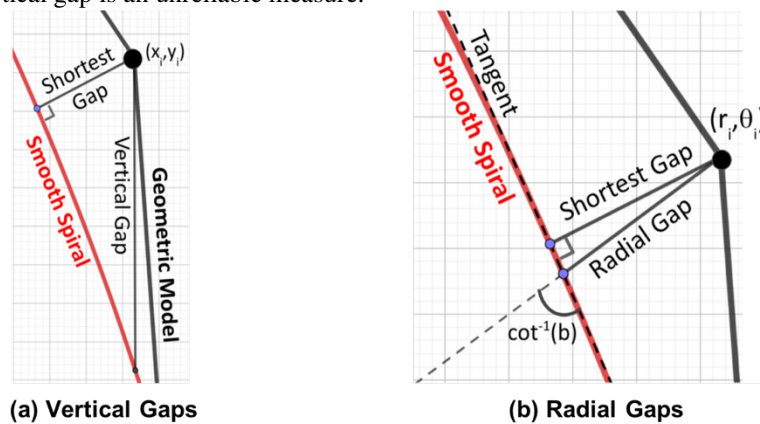

Fig. 10: Vertical, Radial, and Shortest Gaps

Shortest Distance: The actual shortest distance from a vertex is to that point on the smooth curve, such that the line joining the two points makes a right angle with the tangent of the smooth curve (see Figure 10 (a)). However, there is no known closed form formula for the shortest distance between a point (vertex, in our case) and a logarithmic curve [37]. This implies that in order to compute the shortest distance from a given vertex to a logarithmic spiral, we would have to "try out" several points on the logarithmic curve and find the one that is the shortest distance away from the vertex. This can be quite tedious to compute. So, instead, we consider the radial gap, which is a close approximation of the shortest distance, as explained next.

Radial Gap (Polar Coordinates): Logarithmic spirals have a unique property that any radial line to a point on the spiral makes the *same* angle (given by cot^{-1}(b)) with the tangent at that point [30]. From Figure 10 (b), we can see that when cot^{-1}(b) is large (close to 90°), the radial gap is a good approximation for the shortest distance between a vertex and the logarithmic curve. Based on rough fitting by hand, we believe that the best-fitting spiral has a value of b such that cot^{-1}(b) is somewhere between 75°-80°. Hence, we use the radial gap, which is much more efficient to compute than the shortest gap, as a close approximation of the latter.
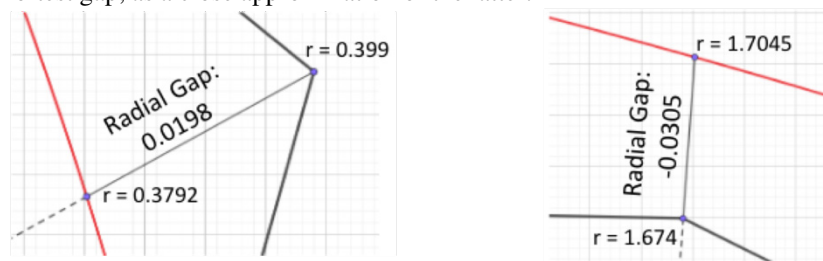

Fig. 11: Radial gaps can be positive or negative

Squaring the Gap: Depending on whether a given vertex of the Geometric Model lies *outside* or *inside* the closest curve of the smooth spiral, the radial gap could be *positive* or *negative*, respectively (Figure 11). If such radial gaps are simply added up, they may cancel each other out, giving the illusion that a given smooth spiral is better fitting than it actually is. However, if we were to compute the *squares* of the radial gaps before adding them, the differences would not cancel out, and would help find the smooth spiral that is actually close to all vertices. This is similar to the least-squares method in curve fitting [31].
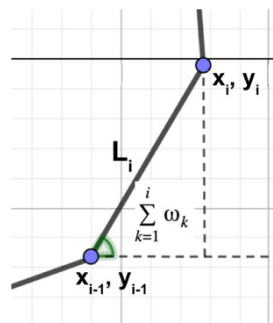
Formulating the Best-Fit Problem

Fig. 12: Deriving x_i, y_i from L_i, ω_i

Deriving Coordinates of the Vertices: In order to compute the radial gap, we need to figure out the polar coordinates of the different vertices of our Geometric Model. For that, we first derive the cartesian coordinates of the vertices from the values of L_i and ω_i, in a recursive manner. We first note that while ω_i is the angle that the ith outer edge makes with respect to the $(i-1)^{th}$ edge, the angle that it makes with respect to the *horizontal* axis, can be computed recursively as: $\sum_{k=1}^{i} \omega_k$. Figure 12 then helps establish the following recursive relations for computing (x_i, y_i) from (x_{i-1}, y_{i-1}):

$$y_i = sin(\sum_{k=1}^{i} \omega_k) * L_i + y_{i-1} \qquad (1)$$

$$x_i = cos\left(\sum_{k=1}^{i} \omega_k\right) * L_i + x_{i-1} \qquad (2)$$

Using $x_0 = y_0 = 0$, we compute all (x_i, y_i). We then translate these coordinates, per the translation vector we are considering (xT, yT). After doing so, we convert each vertex to polar coordinates (r_i, θ_i) using:

$$r_i = \sqrt{(x_i + xT)^2 + (y_i + yT)^2} \qquad (3)$$

$$\theta_i = tan^{-1}\left(\frac{y_i + yT}{x_i + xT}\right) \qquad (4)$$

The Minimization Problem: Given the polar coordinates of the vertices of our translated geometric model, we can then compute the "fit" of a given smooth spiral (defined by a, b), by using the expression: $fitting\ error = \sum_{i=1}^{20}(ae^{b\theta_i} - r_i)^2$.

Given the above, the curve-fitting problem boils down to searching through the space of $\{a, b, xT, yT\}$, to find the combination that yields the lowest value of fitting error. Formally, our goal is to solve the minimization problem below:

$$\min_{\{a,b,xT,yT\}}\left\{\sum_{i=1}^{20}(ae^{b\theta_i} - r_i)^2\right\} \qquad (5)$$

We develop Python code for solving the above numerically.

Are There Additional Local Minima? Our numerical search for a global minimum is more likely to succeed if there are no additional local minima that mislead us in the search space. If not, for a given b, we may conclude that a specific combination of (a, xT, yT) results in the best-fit, while there may be a much better-fitting combination that exists elsewhere.

However, we do not expect local minima to interfere with our search. Here is the intuition for each of the three parameters, a, xT, and yT. First, for a given combination of (b, xT, yT), if we increase (or decrease) the scale factor a from the best fitting value, the logarithmic spiral will grow (or shrink) in size, increasing the radial gap from the vertices of the Geometric Model – the radial gaps will not decrease by further changes in a (therefore, will not result in a local minimum). Second, for a given combination of (b, a), if we increase/decrease the xT and yT from their optimal values, the horizontal and vertical gap (and also, the radial gap) between the logarithmic spiral and geometric spiral vertices will increase – here is no change that will then cause the radial gaps to decrease (and result in a local minimum) with further translation. In short, for each of the parameters a, xT, and yT, as soon as we start deviating from the best-fitting value, the sum of radial gaps will only increase (and not result in local minima). Finally, we limit the search space for the four unknowns based on manually trying out a few different logarithmic spirals and translation vectors – in Section 5, we explicitly validate the above arguments in this limited search space.

The Python Code

We developed a Python program for solving the minimization problem formulated in Section 4.4. In the code screenshot shown above, we calculate the Cartesian coordinates of the vertices for an untranslated geometric model. We convert the vertices to polar coordinates, and compute the sum of the radial gaps for a given combination of a, b, xT, and yT. We iterate over a wide range of values for these four parameters, each with increments of 0.001: $a \in [0.31, 0.34]$, $b \in [0.20, 0.22]$, $xT \in [-0.2, -0.11]$, $yT \in [-0.22, -0.17]$.

Computation Time: We soon realized that if we were to attempt to calculate the best-fitting smooth spiral with a granularity of 0.001 for all the four unknowns, it would take more than 1000 hours for our processing to complete. So, instead, we used a granularity of 0.001 for only a and b, and initially used a coarser granularity of 0.01 for xT and yT. For each value of b, after finding the best-fitting values of (a, xT, yT) using the coarser granularity for the translates, we then conducted a "second" search *around the best-fitting values,* with a finer granularity of 0.001 – this helped us find even better-fitting translation vectors. Our final best-fitting curve was the one obtained after this two-step search. This, in fact, made a huge difference in the computation time, which ended up being only around 26 hours (on a machine with a 2.2 GHz i7 processor, and 8 GB memory).

The Best Fitting Parametric Spiral: Our code found that the following combination of the four unknown parameters yielded the best fitting parametric smooth spiral:

$b \approx 0.207$

$a \approx 0.339$

$xT \approx -0.114$

$yT \approx -0.205$

We note that the scale of a, xT, and yT depends on the side-length, X, of the original origami square. However, b does not depend on X, because it is simply a growth factor, and not a scale or translation factor. For our computations, we used $X = 16$.

The Usefulness of a Parametric Model

The best-fitting Smooth Model we have discovered is a parametric model that is completely characterized by just two parameters (a and b). It is important to note that this model offers significant reduction in the number of parameters over the Geometric Model. The number of parameters in the Geometric model grows linearly as the number of vertices increases, while the smooth approximation can model a spiral with any number of turns, with just a and b. Validation

How Well Does the Parametric Smooth Model Fit the Geometric Model?

In Figure 13, we plot the best-fitting parameter combination for our translated Geometric Model, and the smooth logarithmic spiral. The smooth spiral fits the vertices quite well. It does not touch most vertices, but is fairly close to all and achieves an excellent average of the gaps between all vertices and itself.
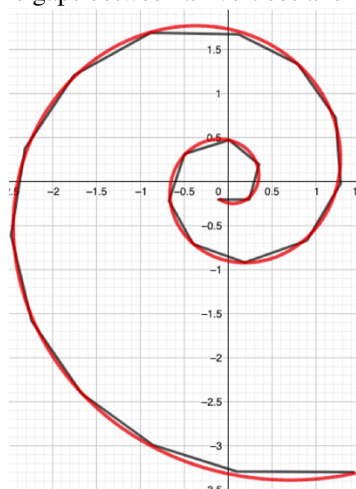

Can We Confirm Absence of Local Minima in Our Search For Best-Fitting Smooth Spirals?

To validate that there are no additional local minima in our search for the best fitting values of a, b, xT, yT, we compute our fitting error as a function of these. We first select the best-fitting a and b found in Section 4.5, and compute the fitting error yielded for different values of xT and yT. Figure 14(a) plots the result (fitting error is normalized). As can be seen, the fitting error is a convex function with respect to xT and yT, and has a clear defined minimum point which confirms that there are no additional local minima.
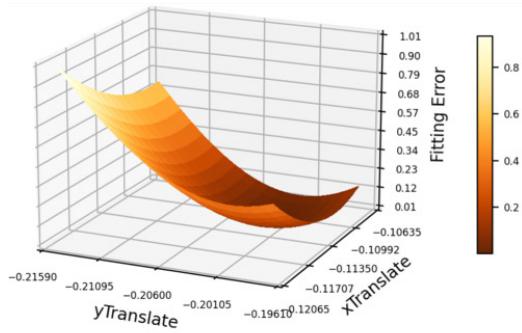
(a) Fitting Error vs. (xT,yT)
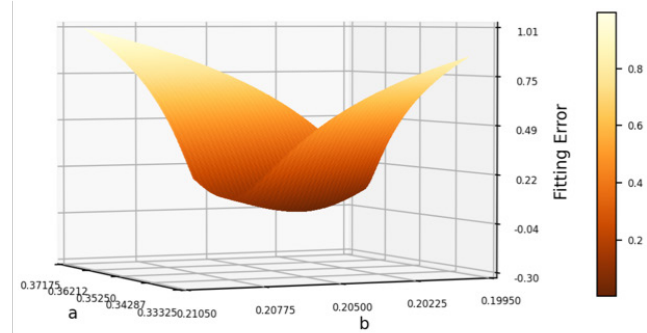
(b) Fitting Error vs. (a,b)

We next study whether the fitting error is also convex with respect to a and b. For each combination of (a, b), we use the translation vector (xT, yT) that yields the smallest fitting error, and then plot the fitting error in Figure 14(b). We observe that this graph too has only one global minimum and is also a convex function. This confirms that our search for a parametric smooth spiral approximation of our Geometric model, truly finds the best fit.

Applications of Our Models

Now that we have mathematical models for the Origami Navel Shell, we apply these to answer several open questions in this section.

Debunking a Claim: Tomoko Fuse's Origami Navel Shell is quite popular and is featured and discussed in many websites. Often, strong claims are made about it. One online blog source that we came across asserted that Fuse's Origami Navel Shell was not a logarithmic spiral, and was not even mathematically precise [23] – our ability to create a very well-fitting smooth logarithmic model for Fuse's design refutes this claim.

How Does the Origami Navel Shell Design Relate to Prior Mathematical Models Proposed for Nautilus Shells?

We use our models to assess whether or not the Origami Navel Shell design is a representative model for Nautilus Shells. In this section, we do this by comparing our models to those found in the literature for the Nautilus Shell. For each model considered in this section, we use a scale factor that lets the inner vertices of our Geometric Model fit it well (and then we assess how well the outer vertices fit). This helps us to get a clear visual and fair comparison of differences between different models.[3]

---

[3] In this subsection, our Geometric and Smooth models are plotted in black and red colors, respectively, while other models are plotted in blue.

(a) Comparison to Golden Spiral   (b) Model from [38]   (c) Model from [14]
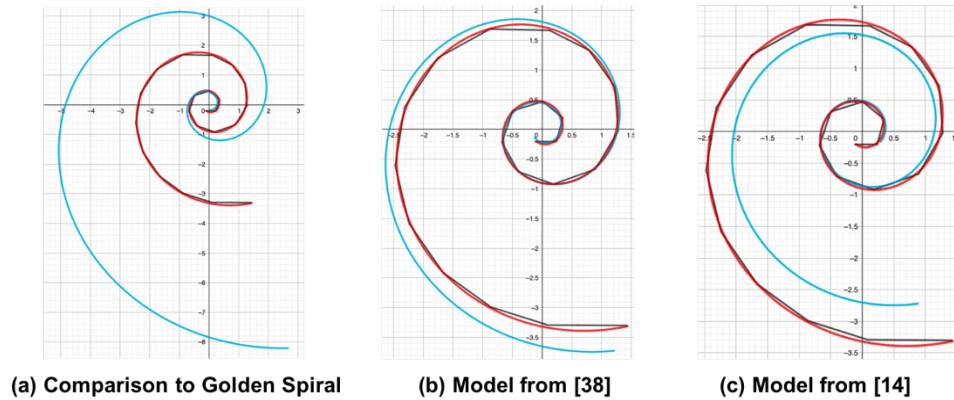
To begin, we wanted to see if the Golden Spiral, which some claim matches the Nautilus shell, would actually fit our model [12][22][34][36]. After fitting the equation of a Golden Spiral ($r = 1.618^{2\theta/\pi}$) onto our smooth curve, we found that it grows much too fast for our Geometric and Smooth Models (Figure 15 (a)). If the Origami Navel Shell indeed is a representative model of the Nautilus Shell in nature, then our findings support the counterclaims in [11][19][26][23][35], that the Nautilus Shell is *not* a Golden Spiral.

Reference [38] proposed this equation for the Nautilus Shell, $r = 1.2(1.25^{\theta})$, but on comparing a scaled version with our models, we found that after fitting the inner curves well, it grew much too fast for our models (see Figure 15 (b)). Reference [14] measures a few different real specimens of the species Nautilus *Pompilius* and found that the growth ratio of different specimens was between 1.24 and 1.43, with the average being 1.33. On comparing a scaled version of the spiral that captures this average ratio, $r = 1.33^{2\theta/\pi}$, we found that when fit well to the inner curves, it grew too slowly for our models (see Figure 15 (c)).

The source [28] states that a growth by the Golden ratio every 90° is too fast for the Nautilus Shell, and 180° is a much better fit. When we compare a scaled version of the corresponding equation $r = 1.618^{\theta/\pi}$ with our models, we find that it grows too slowly and does not fit most of the Geometric Model vertices (see Figure 16(a)).

(a) Model from [28]   (b) Model from [26][28]   (c) First model from [4]   (d) Second model from [4]
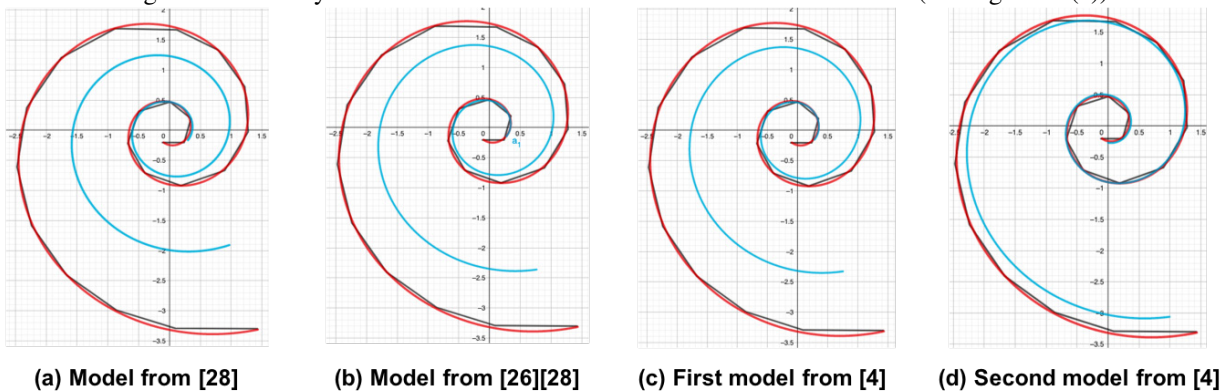
The sources [26] and [28] note that the average spiral corresponding to the 2D cross-section of Nautilus shells, grows by a ratio of 3 every full turn (unlike the Golden Spiral that grows by a ratio of 6.85 every full turn). This boils down to a logarithmic growth rate of $3^{1/4}$ every $\frac{\pi}{2}$ radians. The corresponding spiral equation would be: $r = 1.318^{2\theta/\pi}$. Figure 16(b) compares the scaled version of this to our models. We find that this spiral grows too slowly to fit the outer vertices of the Geometric Model well.

Source [4] relied on measurements of 80 Nautilus specimens from the Smithsonian collection, and found that the average growth ratio for most species was actually 1.31, rather than the 1.33 (= 4/3) reported in [14]. When we

graphed the spiral using a scaled version of the corresponding equation $r = 1.31^{2\theta/\pi}$, we found that when fit to the inner curve well, it grew too slowly for our Smooth and Geometric Models (see Figure 16 (c)). [4] also found that the rare species of Nautilus *Scrobiculatus* had a characteristically different growth ratio of 1.356, the Meta-golden Ratio Chi. The corresponding curve, ($r = 1.31^{2\theta/\pi}$), matched our Geometric and Smooth models the most among all models considered so far (Figure 16 (d)) – however, our models still grow faster.

Can the Ideal Geometric Model Be Used as a Benchmark for Assessing Images of Origami Constructions?

Comparing our Geometric Model of the ideal Origami Navel Shell with images of origami constructions available online gives us many observations regarding how well they fit together. To match our Geometric Model, we attempted to first line up the *outer* vertices of the origami images and our ideal model. We then assessed how well the remaining vertices matched (see Figure 17).
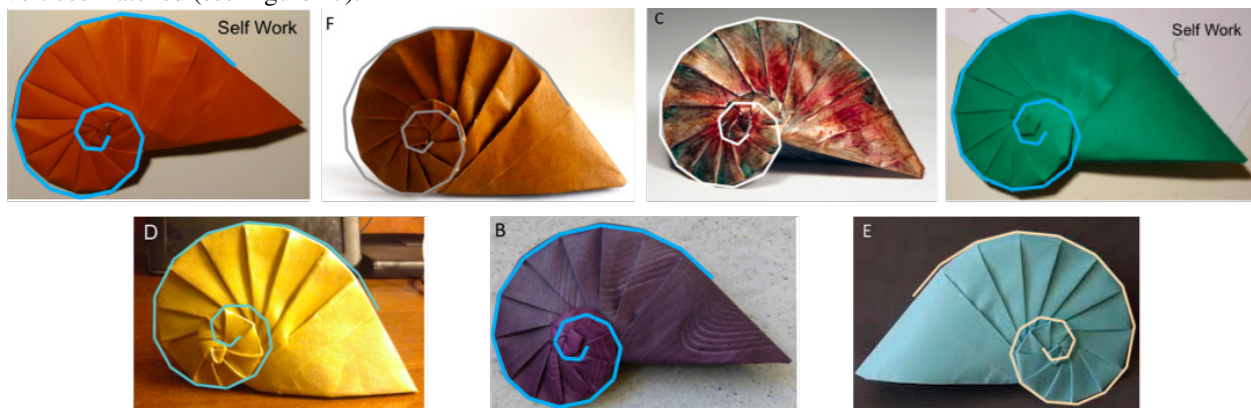

Fig. 17: Our geometric model compared to online/self images of Origami Navel Shells

We find that the outer edges of most origami samples match our ideal Geometric Model quite well; the extent to which the inner and middle edges match, varied across the different photographs. As noted before, we believe this is due to two main factors – the human error involved in the folding process, and the angle and non-orthogonal direction from which the photograph is taken. Our model helped us understand that human and photographic errors impact the *inner* edges of an origami construction more significantly than the outer edges. In some origami images (where the origami structure seems to have been flattened), our model has a good fit with several inner edges as well.

How Closely Does the Origami Navel Shell Model Different Variants of the Nautilus Species?

We collected several online images of the Nautilus shell found in nature, and next studied how well these images match with our best-fitting Smooth Model (Section 4.5). The results are shown in Figures 20 – Figure 18(a) shows the results when we first scale our Smooth Model to try and fit the *outer* curves of the Nautilus image, and then see how well the *inner* curves match; while Figure 18(b) tries to scale the Smooth Model to first fit the *inner* curves well, and then see how well the *outer* curves match.

We find that the degree of match of our Smooth model somewhat differs across different Nautilus images. This is an expected result because of the reported variability across different Nautilus Shells found in nature [28]. Our parametric Smooth Model grows too fast for many Nautilus images. Specifically, when we try to fit the outer curves first, the inner curves do not match well (Figure 18(a)); and when we try to fit the inner curves first, the outer curves do not match well (Figure 18(b)). Both ways, the growth rate of our Smooth Model is greater than that of the

Nautili. Visually, first trying to match the inner curves seems to result in a worse fit (Figure 18(b)), but this could simply be a visual artifact.

The notable exception to the above observation is the last image in the set (bottom-most row in Figure 18) – this image is taken from [4], which studied 80 specimens from the Smithsonian collection; this specific image is that of the rare species of Nautilus *Scrobiculatus*. [4] notes that the growth rate of this variant is notably different from the rest of the specimen. We find that our Smooth Model is a much better match to the image of this specimen, compared to the other variants (for instance, the second-last row is the Nautilus *Pompilius* species). This is also supported by our evaluation in Section 6.1.
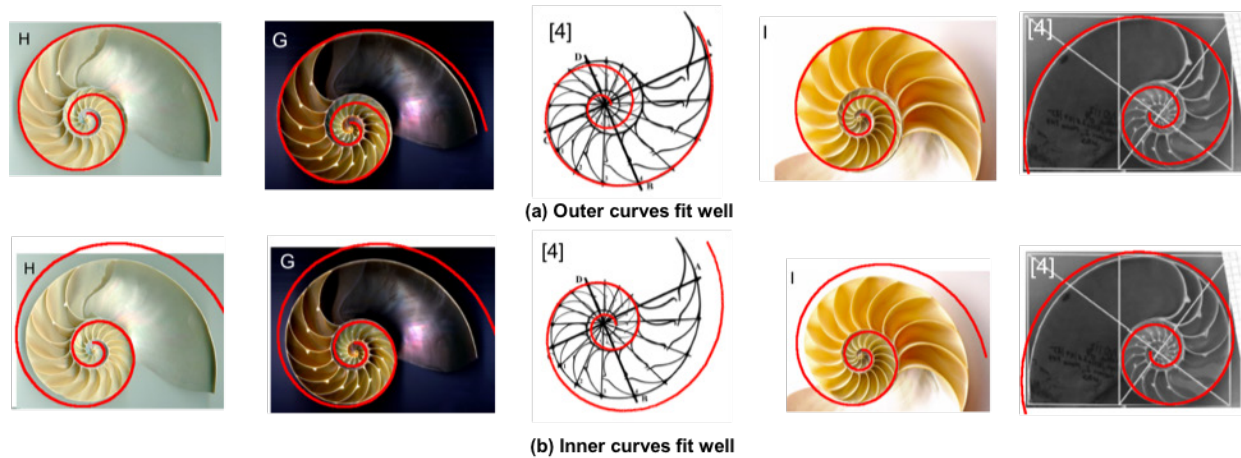

Fig. 18: Our smooth spiral model compared to online images of the Nautilus shell

Discussion

How Do Our Models Relate to Our Observations from Section 3.1?

Recall the questions we raised in Section 3.1, about the possible relation of our two observations (the ratio 4/3, and the Fibonacci Sequence) with the model we develop. In Section 3.1, we had noticed that the Fibonacci Sequence was present in the number of equal-width sections during the folding process and wondered if that may raise the Golden Spiral as a potential candidate for a good fitting spiral. Looking at Figure 15, we know that the Golden Spiral does not fit our Smooth or Geometric models well and grows much too fast with its growth rate of 1.618, φ, every quarter turn. In section 3.1, we also discovered that every equal-width section had edges that were 4/3 (≈ 1.33) as long as the edges in the previous set of equal-width sections. We first tried to draw parallel between the 1.33 ratio and the average growth rate of the Nautilus Shell reported in source [14] as 1.33. However, when we modeled a spiral using 1.33 as the growth rate instead of 1.618, the Golden Ratio, we found that it also did not fit well (Figure 16 (b)).

With some more analysis, we realized that after converting e^b in the logarithmic equation of our best-fitting Smooth Model ($b \approx 0.207$) to the base of 1.618, the equation becomes $r = 1.618^{1.353\,\theta/\pi}$. The number 1.353 is somewhat close to the mysterious ratio of 1.33 we observed in Section 3.1. Is there a relation? We do not know! It may simply be coincidental that the two numbers are similar, but we hope to explore this further in future work.

Limitations of Our Approach

One thing that our research did not help us understand was the relationship between the folding instructions and the growth rate of the Smooth Model – why did the specific growth rate (b) of the Smooth Model we found through parametric curve-fitting, fit the Geometric Model so well? Was there something in the folding instructions that could

have helped us find this *b* value without resorting to curve-fitting? Our methodology so far has not helped us make the connection.

A possible source of error that may have impacted our results would be our decision to *not* use the shortest distance when computing our "fitting metric" (Section 4.3), and instead use the radial gaps for capturing how well fitting the Geometric Model was to a given smooth spiral. However, given the best-fitting smooth spiral we found (*b* ≈ 0.207), the angle made by the radial line with the tangent in Figure 10(b) is 78.3°($= cot^{-1}(b)$). We believe that using the shortest distance instead of the radial gap in this case would not have made a significant difference. Additionally, some of our evaluations could have been impacted because of photography issues. When comparing our Geometric Model to already constructed Origami Navel Shells, the angle that the picture was taken at, could have influenced how well fitting it actually was.

We hope to study the impact of these limitations, along with other future directions identified next.

Future Directions

Our modeling efforts in this project have raised several open issues that could be explored next:

Extending the Geometric Model Beyond 20 Edges: We wonder if the origami design by Tomoko Fuse [16][43] could be extended, can our model help us visualize what an origami spiral with more than 20 edges look like? What would the side lengths be? In our project we stopped at 8, making the length of each folded segment X/16, but if we continued with the next Fibonacci number, 13, how would the angles and side lengths be affected? What would the visual structure look like? Will it still fit the smooth spiral we discovered by curve-fitting?

Evaluating Against Other "Goodness of Fit" Measures: Instead of trying to find the smooth spiral that best fits the *vertices* of the Geometric Model, we could try fitting to the *edges* of the latter. This would involve formulating a different measure for goodness of fit, and re-evaluating the minimization problem. Will the corresponding best-fitting smooth spiral help us discover connections to the folding instructions?

Modeling Other Origami Spiral Designs: We wonder if we could model other origami spirals by analyzing their folding instructions and using a similar process to create a geometric model for them. For instance, reference [44] has a different origami design for a Nautilus Shell, so if we were to model it and create instructions similar to how we did our project, what aspects of our model would change?

Designing Origami Structures for Known Mathematical Spirals: We wonder if our models can help design folding instructions that would lead to origami structures that fit the Golden Spiral well? Can we play around with the angles, widths, and diagonal creases of the folding instructions, in order to achieve the curve of the Golden Spiral? Can we do the same to derive origami designs for other mathematical spirals, including even non-logarithmic spirals?

We hope our research lays the foundation for further research in bridging the gap between origami and mathematical models of spirals. We look forward to witnessing this field grow.

Conclusion

In this paper, we develop and evaluate mathematical models for Tomoko Fuse's Origami Navel Shell, which is believed to be based on the prominent Nautilus Shell. To the best of our knowledge, this has never been done before. Using first-principles geometric and trigonometric constructs, we map Fuse's folding instructions to a precise non-smooth Geometric Model of an ideally-constructed origami spiral. We then rely on a curve fitting approach for finding the closest fitting smooth approximation. By exploiting equiangular properties of logarithmic spirals, we efficiently compute the gap between the Geometric Model and a given smooth spiral, and use it to formulate a minimization problem involving four unknowns. We then design a Python program for numerically searching for the best-fitting smooth logarithmic spiral, as well as for validating the convexity of the minimization problem. We use our two models

to study prior proposed models of the Nautilus, online images of origami shells, as well as images of the different variants of the Nautilus Shell. Our evaluations show that: (i) the Smooth spiral is an excellent fit for the Geometric Model; (ii) our models for Origami Navel Shell are different from prior mathematical models for the Nautilus shell, but they come close to a recent model for a rare species of Nautilus; (iii) the Geometric Model can be used as a benchmark for evaluating construction quality of folded origami spirals, and shows that construction and photographic errors manifest mostly in the inner edges; and (iv) the Smooth Model helps understand how well the ideal Navel Shell matches different variants of the Nautilus species.

Our research lies at the intersection of two important fields. The first is the field of shape modeling, which adds precision, understanding, better designs, and efficiency in several important fields of the scientific world [7][8][32][41]. While the shape of the famed Nautilus shell has been mathematically modeled by many, its origami counterparts have not. We focus on mathematically modeling the shape of Fuse's Origami Navel Shell, and use it for benchmarking and understanding the origami structure as well as for understanding its relationship with Nautilus Shells. Our spiral models can also serve as benchmarks against other models developed by mathematicians and origamists. We hope that, in future, our models aid biologists in better understanding the physical and biological processes that determine the shape of a Nautilus's shell.

The second field impacted by our research is that of origami. Since the middle of the 20th century, there has been a significant jump in the application of origami for solving problems in mathematics, science, engineering, and education. Origami solutions are simpler to develop than most scientific theorems. Different properties, such as shape, dimensions, and surface area, allow a device based on a single origami pattern to do multiple functions [3]. For instance, origami has been used in applied math and engineering (such as folding telescopes and airbags, circle packing, models of bridges and stadiums, modeling DNA samples, and space technology), problem solving and shape modeling using paper folds and cuts [1][2][24][10]. So far, the mathematics of origami has mostly focused on studying properties (such as flat-foldability) of origami models, or using paper folds to solve mathematical equations [9][17][21].

Origamists have also specifically taken a keen interest in the Nautilus Shell, just like mathematicians have. Indeed, several different origami structures have been designed, based on the Nautilus. However, the mathematical modeling of such origami spirals has been mostly ignored. We have picked one of the most prominent of these origami structures, and have successfully derived mathematical models for it. We hope that this success encourages further work on developing a formal framework for mapping folding instructions, geometric models, and smooth spirals.

Photo Credits

A	https://www.pinterest.com/pin/421860690091943911/
B	https://www.flickriver.com/photos/tags/navelshell/interesting/
C	https://origami.me/seashells/
D	https://www.deviantart.com/naganeboshni/art/Navel-Shell-Golden-Painted-Edition-381513478
E	https://www.youtube.com/watch?app=desktop&v=I5Kzi4X_G1s
F	https://www.youtube.com/watch?v=cBEQMXKtpP4
G	https://br.pinterest.com/pin/422494008796579446/
H	https://www.americanscientist.org/article/twisted-math-and-beautiful-geometry
I	https://br.pinterest.com/pin/422494008796579446/

Acknowledgements

Bibliography

American Institute of Physics. "Origami Helps Scientists Solve Problems." ScienceDaily. ScienceDaily, Feb 2002, https://www.sciencedaily.com/releases/2002/02/020219080203.htm. Accessed 7 Dec 2020.

Asiel, Fatma. "Origami Applications in the Past and Present." Bibalex, 5 Dec 2017, https://www.bibalex.org/SCI-planet/en/Article/Details?id=10309. Accessed 9 Dec 2020.

Avila, A., Magleby, S. P., Lang, R. J., and Howell, L. L.: Origami fold states: concept and design tool, Mech. Sci., 10, 91–105, 2019.

Bartlett, Christopher. "Nautilus Spirals and the Meta-Golden Ratio Chi." *Nexus Network Journal*, vol. 20, no. 3, 2018, p. 279.

Borcherds, M. "GeoGebra Classic." 2001, https://www.geogebra.org/classic.
Brown, Dan. The Da Vinci Code. 2003, USA. New York: Doubleday.

Chu, Jennifer. "Here Comes the Sun. " *MIT News*, 2012, https://news.mit.edu/2012/sunflower-concentrated-solar-0111. Accessed 5 Dec 2020.

Dai, H., Pears, N., Smith, W. et al. "Statistical Modeling of Craniofacial Shape and Texture". International Journal of Computer Vision, 128, 547–571, 2020.

Demaine, Erik D.; O'Rourke, Joseph Geometric folding algorithms. 2007, Cambridge: Cambridge University Press. doi:10.1017/CBO9780511735172.Demaine, Erik D.; O'Rourke, Joseph Geometric folding algorithms. 2007, Cambridge: Cambridge University Press. ISBN 978-0-521-85757-4. MR 2354878.

Demaine, Erik. "Erik Demaine's Folding and Unfolding Page." *Erik Demaine*, 2020, http://erikdemaine.org/folding/. Accessed 4 Dec 2020.

Delvin, Keith. "The Man of Numbers: in Search of Leonardo Fibonacci." *The Man of Numbers*, 2010, https://www.maa.org/external_archive/devlin/Fibonacci.pdf. accessed 6 Dec 2020.

Devlin, Keith. The Myth That Will Not Go Away. 2007, https://www.maa.org/external_archive/devlin/devangle.html. Accessed 6 Dec 2020.

Du Sautoy, M. The Secrets of the Nautilus Shell - The Code. Episode 1, BBC Two, 2011. https://www.youtube.com/watch?v=Ysw3iM3ENQA. Accessed 6 Dec 2020.

Falbo, Clement. The Golden Ratio—A Contrary Viewpoint. The College Mathematics Journal. 36, 2005.

Fletcher, R. Proportion and the Living World. Parabola 13(1): 36-51, 1988.

Fuse, Tomoko. *Spiral Origami Art Design*. Viereck Verlag, 2012.

Geretschläger, Robert. Geometric Origami. 2008, UK: Arbelos. ISBN 978-0-9555477-1-3.
Happy Folding. *Navel Shell (Tomoko Fuse) Instructions.* https://www.happyfolding.com/instructions-fuse-navel_shell. Accessed 5 Dec 2020.

Hart, George W. "Replicator Constructions." *Replicator Constructions*, 2010, http://www.georgehart.com/rp/replicator/replicator.html. Accessed 6 Dec 2020.

Impens, C. Debunking golden ratio shells, 1 & 2. Chris Impens @ Valvas, 2016, http://ci47.blogspot.be/2016/08/debunking-golden-ratio-shells-1.html. Accessed 5 Dec 2020.

Lang, Robert J. "From Flapping Birds to Space Telescopes: The Modern Science of Origami". Usenix Conference, Boston, MA, 2008.

Livio, M. The Golden Ratio: The Story of PHI, the World's Most Astonishing Number. 2003, Crown, New York: Broadway.

long_quach. "Nautilus." *Neorigami*, 2013, https://neorigami.com/neo/index.php/en/geometric-a-abstract/item/6916-nautilus. Accessed 6 Dec 2020.

Malkevitch, Joseph. Mathematics and Art. Feature Column, American Mathematical Society, 2003, http://www.ams.org/publicoutreach/feature-column/fcarc-art1 . Accessed 5 Dec 2020.

Maor, Eli, and Eugen Jost. "Twisted Math and Beautiful Geometry." *American Scientist*, Volume 102, Number 2, 2014.

Math Tourist. "Sea Shell Spirals." *The Mathematical Tourist*, 2020, http://mathtourist.blogspot.com/2020/06/. Accessed 5 Dec 2020.

McMahon, T. A. and J. T. Bonner. On Size and Life. 1983, New York: Scientific American Books, 1st Edition.

Meisner, Gary. "Is the Nautilus Shell Spiral a Golden Spiral?" *GoldenNumber.net*, 2014, https://www.goldennumber.net/nautilus-spiral-golden-ratio/. Accessed 5 Dec 2020.

Meisner, Gary. "Spirals and the Golden Ratio." *The Golden Number*, 2012, https://www.goldennumber.net/spirals/. Accessed 6 Dec 2020.

Mukhopadhyay, Utpal. "Logarithmic Spiral-A Splendid Curve." *Resonance*. 9. P. 39-45. 10.1007/BF02834971, 2004.

Quarteroni, A., Saleri, F., Gervasio, P., "Scientific computing with MATLAB and Octave". 4th edition, 2014, Springer-Verlag Berlin Heidelberg.

Rogers, Kara. "Scientific Modeling." *Britannica*, 2012, https://www.britannica.com/science/scientific-modeling. Accessed 7 Dec 2020.

Rusczyk, Richard. Art of Problem Solving Introduction to Geometry. vol. 2, Aops, Incorporated, 2013.
Ryan, M. Geometry for Dummies. Hoboken: Wiley, 2016.

Sharp, John. "Spirals and the Golden Section." *Nexus Network Journal*, vol. 4, no. 1, p. 59-82, 2002.
Smithsonian Ocean Portal website. https://ocean.si.edu/ocean-life/invertebrates/couple-nautiluses. Accessed 8 Dec 2020.

StackExchange. "Distance between a point and a spiral." September 2013, https://math.stackexchange.com/questions/175106/distance-between-point-and-a-spiral. Accessed 9 Dec 2020.

Strang, Gilbert, and Edwin Herman. "10.3: Polar Coordinates." *LibreTexts*, 2019, https://math.libretexts.org/Courses/University_of_California_Davis/UCD_Mat_21C%3A_Multivariate_Calculus/10%3A_Parametric_Equations_and_Polar_Coordinates/10.3%3A_Polar_Coordinates. Accessed 5 Dec 2020.

Strogatz, S. Me, Myself and Math, Proportion Control. 2012, https://opinionator.blogs.nytimes.com/2012/09/24/proportion-control/. Accessed 5 Dec 2020.

Thompson, D'Arcy. On Growth and Form: The Complete Revised Edition. 1992, New York: Dover Publications.
UCSF Department of Radiology & Biomedical Imaging. "Benefits of Imaging using Radiation." *UCSF*, 2015, https://radiology.ucsf.edu/patient-care/patient-safety/radiation-safety/benefits. Accessed 7 Dec 2020.

Wikipedia. "Spiral." *Wikipedia*, 2020, https://en.wikipedia.org/wiki/Spiral. Accessed 5 Dec 2020.

Wonko. "276: Nautilus." *Setting the Crease*, http://www.wonko.info/365origami/?p=1797, 2011. Accessed 6 Dec 2020.

Zodl, Evan. "Nautilus." *EZ Origami*, 2016, https://ez-origami.com/original/nautilus/. Accessed 5 Dec 2020.